

2021

Shear Behavior of High-Performance Reinforced Concrete Beams

Eman Wehdan, Salah Taher, hamdy afefy, Nesreen Kassem

Follow this and additional works at: <https://digitalcommons.aaru.edu.jo/erjeng>

Recommended Citation

Wehdan, Salah Taher, hamdy afefy, Nesreen Kassem, Eman (2021) "Shear Behavior of High-Performance Reinforced Concrete Beams," *Journal of Engineering Research*: Vol. 5: Iss. 3, Article 3.
Available at: <https://digitalcommons.aaru.edu.jo/erjeng/vol5/iss3/3>

This Article is brought to you for free and open access by Arab Journals Platform. It has been accepted for inclusion in Journal of Engineering Research by an authorized editor. The journal is hosted on [Digital Commons](#), an Elsevier platform. For more information, please contact rakan@aar.edu.jo, marah@aar.edu.jo, u.murad@aar.edu.jo.

Shear Behavior of High-Performance Reinforced Concrete Beams

Salah El-Din F. Taher¹, Hamdy M. Afefy^{1,2}, Nesreen M. Kassem¹ and Eman Wahdan¹

¹Structural Engineering Department, Tanta University, Tanta, Egypt.

²Construction Engineering and Management, Pharos University, Alexandria

E-mail: salah.taher@f-eng.tanta.edu.eg, hamdy.afefy@pua.edu.eg, hamdy.afefy@f-eng.tanta.edu.eg, nesress.kassem@f-eng.tanta.edu.eg, emanwahdan2016@yahoo.com

Abstract:

High-performance concrete (HPC) is one of such new material that has a major improvement over conventional concrete; however, its behavior has to be fully understood. This paper presents experimental and numerical investigations in order to study the shear behavior of high-performance reinforced concrete beams. Four RC-HPC beams were tested experimentally in order to study the effect of the existence of web reinforcement and bar diameter of the web reinforcement as well as the amount of the tensile longitudinal steel bars on the shear behavior. Test results showed higher values of shear strength, stiffness, ductility and controlled the concrete cracking behavior due to the presence of stirrups. The ultimate load for beam having shear reinforcement of 6 mm diameter increased by about 16% compared to that of control beam BI-1 without shear reinforcement, while, that increase reached up to 34% for beam having 8 mm diameter web reinforcement. Besides, the numerical modeling enabled to capture satisfactory the behavior of HPC beam so that it can be used to study the effect of more parameters on the behavior of HPC beams.

1. INTRODUCTION

While reinforced concrete can carry high stresses under compression, it proved to be cracked easily under tensile stresses. The development of cracks does not only affect the aesthetics of the structures but also exposes the steel reinforcement to corrosion. Concrete with compressive strength greater than 50 MPa proved to behave in a very brittle manner. Therefore, the addition of fibers to concrete in order to reduce the brittleness was studied since the 1980's. The fibers have additional positive effects on the concrete such as; increased compressive and tensile strength and enhanced post-cracking characteristics. Over the years, there has been substantial development in the field of fiber reinforced concrete. Fiber reinforced concrete is made with various types of fiber materials, such as carbon, nylon and polypropylene. In particular, this had inspired many researchers to study the possibility of type of steel fiber reinforcement. Steel fiber has many defects such as low workability, high cost and corrosion. Nonmetallic fibers such as polypropylene fiber have attracted great interests to improve the defect of steel fiber. Shear failure mechanism in reinforced concrete structure is known to be complicated and several factors affect it. Taylor [1], conducted tests on reinforced concrete beams without shear reinforcement in order to study the effect of concrete strength on shear capacity. It was concluded that the diagonal cracking load improved with increase in the strength of the concrete. Ghadhban [2] and Mohamed Zakaria et al. [3] showed that increasing the longitudinal reinforcement ratio

resulted in increased in relative shear strength value. The larger amounts of longitudinal reinforcement cause smaller spacing's between shear cracks, and thus result in smaller shear crack widths. Piyamahant [4] concluded that small amount of web reinforcement is sufficient to improve the shear carrying capacity. Birtel and Mark [5] studied the shear failure of RC beams using nonlinear finite element analysis. The results showed that additional horizontally oriented stirrups in cases of distributed longitudinal bars help to reduce lateral deformation and increase bearing capacities. Naik and Kute [6] tested 54 deep beams (9 control specimens without fibers and shear reinforcement), 27 SFRC deep beams with longitudinal steel ratio of 1% and crimped steel fibers having volume fractions of (0.5, 1.0, 1.5%) and 18 beams having varying longitudinal steel and shear reinforcement. It was observed that the increase in shear span to depth ratio causes decrease in shear strength of deep beams. Elzanaty et al. [7] tested 18 beams made of HSC. It was observed that the shear strength of the test beams decreased with increasing a/d ratio. The shear strength of concrete has inverse relation with the depth of the beam. Chana [8], tested various beam scaled down size with proportionally scaled down coarse aggregate. It was observed that small-scale beams were relatively stronger in shear than large-scale beams. Haidar and Perooz [9], carried out experimental and numerical investigations focused on enhancing the shear resistance of reinforced concrete beams using a suitable fiber dosage, and the use of UHPC. The experimental results confirmed that using the fiber in UHPC beams would increase the shear strength and the ductility. Replacing stirrups completely with fibers, led to a reduction of beam depth as well as a decrease in stirrup assembly time. Swamy et al. [10], showed that adding fibers reduced width and numbers of cracks and increased shear strength. Dinh [11], carried out an experimental investigation to study the use of fibers as a replacement to shear reinforcement. It was observed that inclusion of fibers decreased crack width and controlled the concrete cracking. In this study, experimental and numerical program was undertaken with the goal of generating required information in order to understand shear behavior of HPC beams.

2. EXPERIMENTAL WORK

2.1 Test specimens

Experimental tests were conducted on four simply supported HPC beams having rectangular cross-section of 100 mm width by 150 mm total depth. The total length and center-to-center spans of the beams were 1000 and 900 mm, respectively. The first beam BI-1 was reinforced without shear reinforcement; however, the longitudinal tensile steel reinforcing bars were two bars of 16-mm diameter. Beam

BII-1 had shear reinforcement consisted of 6-mm diameter and arranged at 150 mm spacing, while the tensile reinforcement was the same as that of beam BI-1. For this beam, two deferment steel bars of 10 mm diameter were used as upper reinforcement. Beam BIII-1 had the same longitudinal and transversal reinforcement as those of beam BII-1 except that the diameter of shear reinforcement was increased to be 8 mm. Beam BIV-1 was similar to beam BIII-1 except that the diameter of the lower steel bars was reduced to be 12 mm. Figures 1 to 4 show the sectional elevation and cross-section for the four beams, respectively.

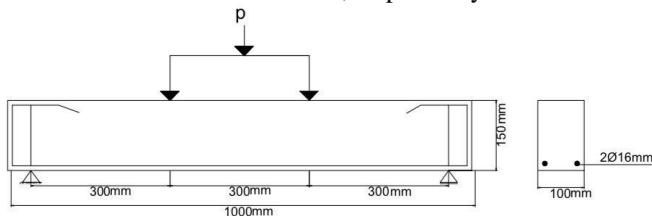


Fig. 1: Typical section of beam BI-1.

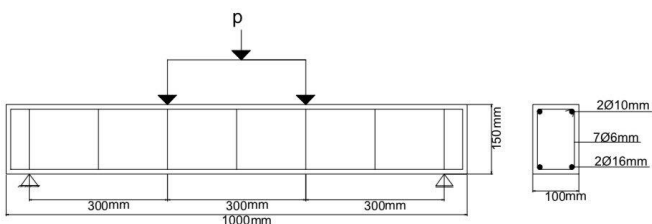


Fig. 2: Typical section of beam BII-1.

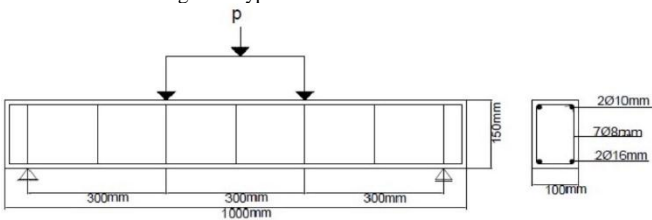


Fig. 3: Typical section of beam BIII-1.

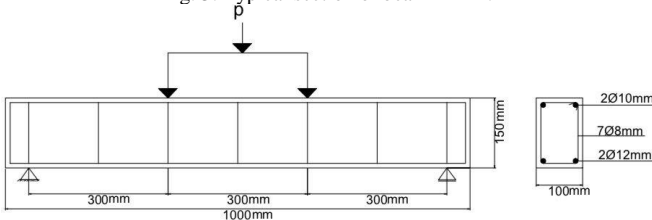


Fig. 4: Typical section of beam BIV-1.

2.2 Materials and Mixture Proportions

HPC consists of cement, silica fume, sand, fibers, water and super plasticizer. The used water/cement-ratio was 0.35, while 10% of the used cement was replaced by silica fume. Silica fume is added to Portland cement concrete to improve its properties, in particular its compressive strength, bond strength, and abrasion resistance. The cement content was 450 kg/m³. The basalt aggregates are higher in specific gravity and lower in absorption and abrasion loss values. Therefore, basalt is most likely to be used in concrete mixes. Graded crushed basalt with maximum nominal particle size of 19 mm was used. Natural sand was used as fine aggregates. Silica is an ultrafine material with spherical particles less than 1 μm in

diameter, the average being about 0.15 μm. This makes it approximately 100 times smaller than the average cement particle. Polypropylene fiber was used for specimens because of its low specific gravity (0.90 – 0.91 gm/ cm³). Polypropylene yields the greatest volume of fiber for a given weight. This high yield means that polypropylene fiber provides good bulk and cover, while being lighter in weight. Using fibers lead to high tensile strength, better energy absorption, larger ductility, and durability. Super plasticizers addition to concrete allows the reduction of the water to cement ratio without negatively affecting the workability of the mixture, and enables the production of high performance concrete. The strength of concrete increases when the water to cement ratio decreases. However, their working mechanisms lack a full understanding, revealing in certain cases cement-superplasticizer incompatibilities. An optimal super plasticizer/silica fume ratio 1: 2.27 was used to achieve good workability.

A concrete mix was designed to have 28-day (f_{cu}) concrete compressive cube strength equals to 45 MPa. For each specimen, three standard concrete cubes of 150 mm side length were prepared and tested in order to estimate the actual concrete strength at the testing day. Table 1 shows the concrete mix properties. From the same concrete mix, three standard cylinders of size 150 x 300 were prepared in order to estimate the actual concrete indirect tensile strength after 28 day. The average indirect tensile strength was found to be 4.1 MPa.

TABLE 1. The concrete mix properties

Coarse aggregate (kg/ m ³)	900
Fine aggregate (kg/ m ³)	900
Cement (kg/ m ³)	450
w/c ratio	0.35
Silica fume (kg/ m ³)	45
Superplasticizer (kg/ m ³)	19.8
Polypropylene fibers(% volume)	0.7%

2.3 Description of the test set-up

All tested beams were loaded symmetrically with two equal concentrated loads as shown in Fig. 5. All beams were fully instrumented to measure the applied loads on the beams, the deflections and strain in longitudinal steel bars. The acting load was measured by a load cell of 1000 kN capacity.



Fig. 5: Test setup for specimens.

3. TEST RESULTS

The test results for all beams were summarized in tables and graphical forms. These results included the maximum loads, crack pattern and modes of failure, load-deflection behavior, and strain in the longitudinal reinforcement, strains

in web reinforcement. These results are discussed in the subsequent sections.

3.1 Cracking and ultimate loads

The results of tested beams are summarized in Table 2, which include flexural cracking load, the load at initiate of the inclined shear crack (diagonal cracking load), the failure load (ultimate load) and the mid span deflection. Fig. 6 shows comparisons among the different loads for all beams. Beam BIII-1 with shear reinforcement 8-mm diameter had the highest diagonal cracking and the highest ultimate loads. It was observed that providing of web reinforcement resulted in increase the ultimate load. The ultimate load for beam BII-1 having shear reinforcement of 6mm increased by about 16% compared to that of beam BI-1 without shear reinforcement. This increase reached up to 34% for beam BIII-1 when the bar diameter increased to be 8 mm.

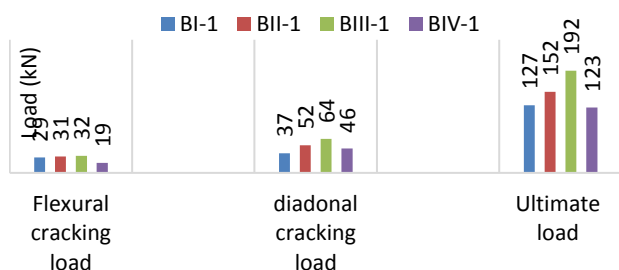


Fig. 6: Flexural cracking, critical shear crack and ultimate loads for the tested beams.

TABLE 2. Main results obtained from experimental work

Beam	BI-1	BII-1	BIII-1	BIV-1
Flexural cracking load (kN)	29	31	32	19
Diagonal cracking load (kN)	37	52	64	46
Ultimate load (kN)	127	152	192	123
Mid-span deflection at ultimate load (mm)	3.41	4.86	5.32	5.63

3.2 Crack Pattern and Modes of Failure

All cracks were marked on the tested beam during the loading course and up to failure. The value of the applied load was inscribed at the extent of each crack at that load level. In this way, a complete crack propagation history was available from image taken at the end of the test. The development of cracks provided information regarding the failure mechanism of the beam. All beams were loaded symmetrically with two equal concentrated loads. During testing, the cracks were marked and beams were photographed. Crack pattern for the tested beams are shown in Figs. (7 to 10).

The flexural cracks initiated in the region of pure flexure and extended vertically. With increased load, more flexural cracks were developed in middle part and the shear span regions of the beam. Cracks in the pure moment region were almost vertical, while those in the shear span zone inclined between the point of the applied load and the support point. At a certain point after the formation of most of flexural

cracks in all beams, an inclined shear crack started to propagate in one shear span or simultaneously in both shear spans. Shortly after the major shear crack formed, a small diagonal crack appeared suddenly slightly above the main steel level and at approximately the middle of the shear span. As the load increased, the initiated inclined shear crack extended further towards the loading points and the supports till complete shear failure occurred.

3.3 Load-deflection Behavior

The load-deflection curves of all tested beams with and without stirrups are shown in Fig. 11. It is obviously that all beams had a similar trend.



Fig. 7: Final crack pattern of beam BI-1.



Fig. 8: Final crack pattern of beam BII-1.



Fig. 9: Final crack pattern of beam BIII-1.



Fig. 10: Final crack pattern of beam BIV-1.

Until the first diagonal cracking load-deflection, curves show linear relationship, and after that, it started to become nonlinear. As the load increased, additional diagonal cracks were developed and significant redistribution of stresses and strains occurred led to a decrease in beam stiffness. From Fig. 11, it can be observed that placement of web reinforcement resulted in increase the stiffness of the beam. The combined effect of using vertical stirrups and HPC enhanced the post-peak load-deflection plateau.

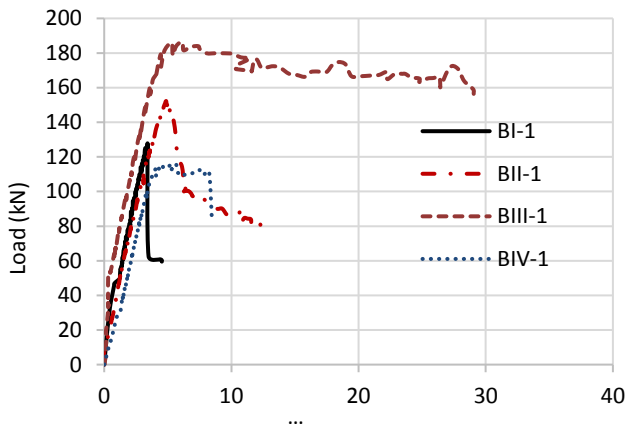


Fig. 11: Load-deflection curves for UHPFRC specimens

4. NUMERICAL MODELLING

In general, the scope of using an experimental approach for investigation is limited. The data required for a comprehensive parametric study is normally inadmissible in an experimental program as the cost and time of conducting an extensive number of experiential tests would be prohibitive. Comprehensive data normally obtained using a suitable numerical technique. Therefore, the finite element method is usually appropriate to generate more parametric data. ABAQUS software package was selectively used to simulate the behavior of the four beams tested in experimental study.

In this study, 8-node (hexahedral), tri-linear displacement, reduced integration, hourglass control C3D8R element, is used to model concrete. For the studied beams, the reinforcing steel is modeled as individual truss elements with steel material properties and cross sections. These truss elements are embedded in the concrete by constrain called embedded region, available in ABAQUS program. The element T3D2 (2-node linear displacement) is used to model reinforcing bars (ABAQUS, 2013).

4.1 Material Properties

4.1.1 Concrete

ABAQUS has three models for modeling the nonlinear behavior of concrete. The plastic damage model is selected for this study assuming that tensile cracking and compressive crushing are the main two failure mechanisms of the concrete material. The five plastic damage parameters are the dilation angle, the flow potential eccentricity, the ratio of initial biaxial compressive yield stress to initial uniaxial compressive yield stress, the ratio of the second stress invariant on the tensile meridian to that on the compressive meridian and the viscosity

parameter that defines viscoplastic regularization. The values of the last four parameters recommended by the ABAQUS documentation for defining concrete material and were set to 0.1, 1.16, 0.66, and 0.0, respectively. The dilation angle and Poisson's ratio were chosen to be 37° and 0.2, respectively.

The elastic modulus of high-performance concrete estimated according to the Egyptian code of practice ECP 203-2018 [12] by the following:

$$E_c = 4400 \sqrt{f_{cu}}$$

The initial tangent modulus of high strength concrete estimated by Carreira and Chu's Model (1985) by the following:

$$E_{it} = (f_c')^{1/3}$$

4.1.2 Steel reinforcement

The steel is assumed to be bilinear elastic-plastic material. Perfect bond is assumed between the steel and concrete. The essential input parameters for material definition of steel bars, contains density, elastic and plastic behavior. Elastic behavior of steel material is defined by specifying Young's modulus (E_s) and Poisson's ratio (ν) of which typical values are 2×10^5 MPa and 0.3, respectively.

4.2 Verification of finite element model

To verify the finite element model of the HPC beam, one beam from other experimental study (Ahmed T. Baraghith et al. [13]) was simulated. The beam assessed the performance of HPC beam under two-point load. The yield stresses of the longitudinal and transverse reinforcement for the chosen beam BHS3.5, 0 were 410 MPa and 250MPa, respectively. In addition, the concrete cube compressive strength of the beam was about 61.4 MPa. The results from the FEM analysis were then compared with the experimental results. The load-deflection curves for beam are shown in Fig. 12. In the linear part, the FEM results are slightly stiffer than the experimental results. One explanation for this may be the assumption of perfect bond between concrete and steel. The FEM model also shows good agreement with the experimental work in the developed failure mode as shown in Fig. 13.

5. FEM RESULTS COMPARED WITH EXPERIMENTAL DATA

All numerical models have predicted the ultimate load and represented well the nonlinear load-deflection response up to the ultimate load. The numerical load-deflection curves are slightly stiffer than the experimental curves.

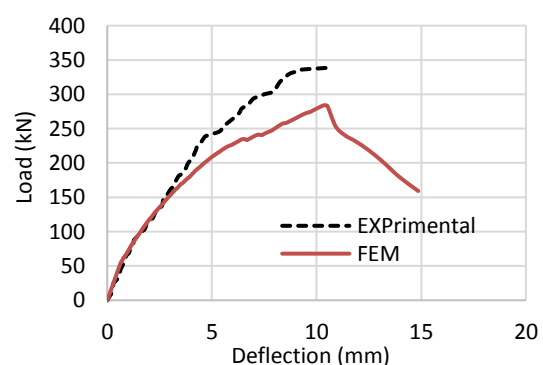


Fig. 12: Comparison between the experimental and the FE analysis results.

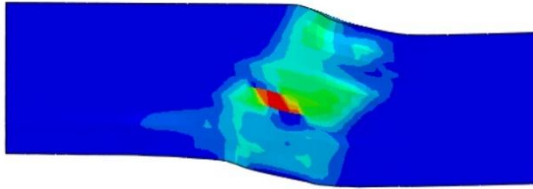
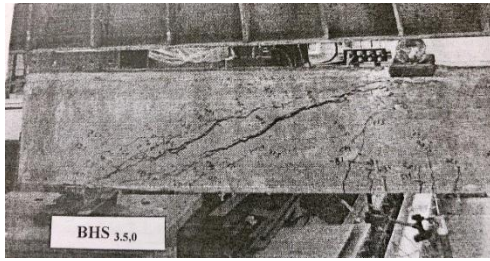


Fig. 13: Experimental and numerical failure mechanism of specimen BHS3.5,0

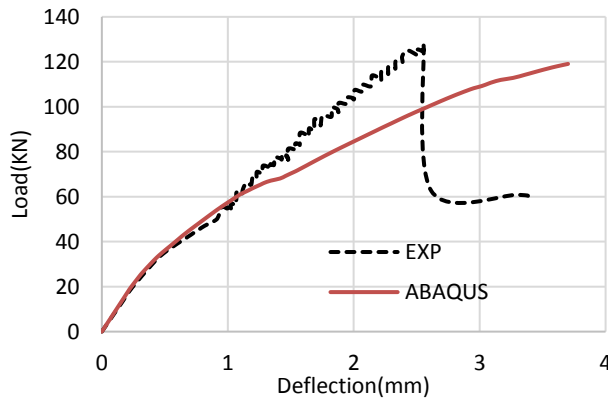


Fig. 14: Load-deflection curves for BI-1 specimen

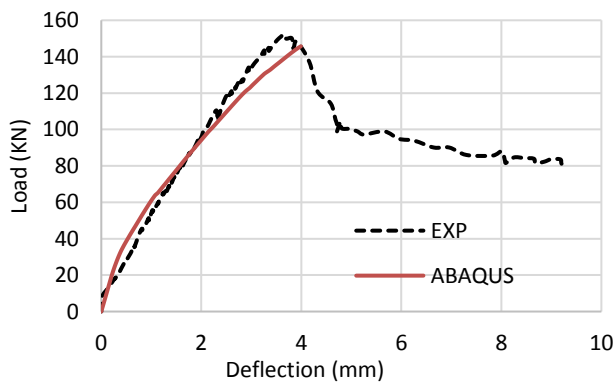


Fig. 15: Load-deflection curves for BII-1 specimen

6. CONCLUSIONS

In the current study, shear performance of high-performance reinforced concrete beams have been investigated. Based on the geometry of the tested beams, the following conclusions are drawn:

- 1) The use of HPC led to an improvement in cracking behavior, which was evidenced by better control of crack widths.

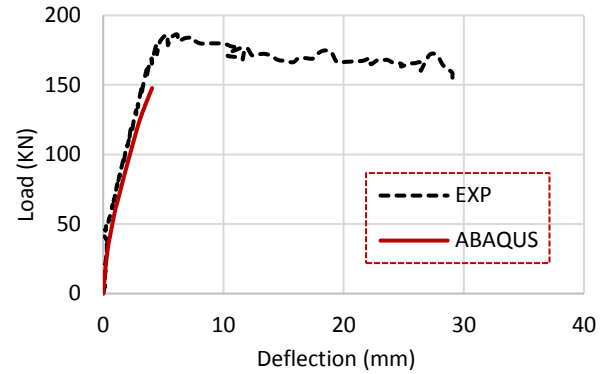


Fig. 16: Load-deflection curves for BIII-1 specimen

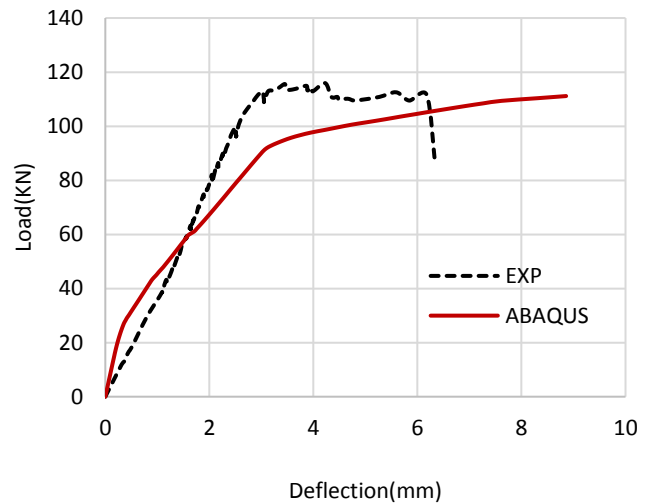


Fig. 17: Load-deflection curves for BIII-1 specimen

- 2) The use of web reinforcement in HPC beams led to an improvement in cracking behavior. Using of web reinforcement resulted in increases the ultimate load. The ultimate load for beam BII-1 having shear reinforcement of 6mm increased by about 16% compared to that of beam BI-1 without shear reinforcement. This increase reached up to 34% for beam BIII-1 when the bar diameter increased to be 8 mm.

REFERENCES

- [1] R. Taylor, (1960), " Some shear tests on reinforced concrete beams without shear reinforcement", Magazine of Concrete Research, Vol 12, No 36, November 1960, pp. 145-154.
- [2] Hadi Nasir Ghadhban, (2007), "Effect of Beam Size on Shear Strength of Reinforced Concrete Normal Beam", Journal of Engineering and Development, Vol. 11, No. 1, March (2007).
- [3] Mohamed Zakaria ,Tamon Ueda, Zhimin Wu and Liang Meng, (2009), " Experimental Investigation on Shear Cracking Behavior in Reinforced Concrete Beams with Shear Reinforcement" Journal of Advanced Concrete Technology Vol. 7, No. 1, 79-96, February 2009
- [4] Piyamahant, (2002), " Shear behavior of reinforced concrete beams with small amount of web reinforcement", M. Eng. Dissertation, Kochi University of Technology, Japan
- [5] V.Birtel, P. Mark, (2007). " Parameterised finite element modelling of RC beam shear failure". In ABAQUS users' conference, (pp. 95–108).
- [6] Dr. Uday P. Naik, Dr. Sunil Y. Kute, (2017), "Use of Steel Fibers as Shear Reinforcement for Deep Beams in Shear- an Experimental

- Study" ,International Journal of Engineering Science and Computing, , Volume 7 , No.7, July 2017
- [7] Ashraf H. Elzanaty, Arthur H. Nilson, and Floyd O. Slate ,(1986)," Shear Capacity of Reinforced Concrete Beams Using High-Strength Concrete", Report No.85-1, Dept. Of structural Engineering, Cornell University, Ithaca, N.Y.
- [8] Chana,(1981) ,"some aspects of modeling the behavior of reinforced concrete under shear loading ",Technical Report No.543,Cement and Concrete Association, Wexham Springs,UK,PP1-22
- [9] Haidar Hosamo and Perooz Sarwari, (2019)," Experimental and finite element analysis of the shear behaviour of UHPC beams", MSc Byggdesign .May2019
- [10] Swamy ,R.N,Jones,R.,and CHIAM,T,(1989) ,"Shear transfer in steel fiber reinforced concrete ",ACI,SP-105 ,PP.565-592.
- [11] DINH, H.H. (2010),"Shear behavior of steel fiber-reinforced concrete beams without stirrup reinforcement ", ACI Structural Journal, vol.107, n.5, p.597-60.
- [12] Egyptian Code of Practice: ECP 203-2018, "Design and Construction for Reinforced Concrete Structures," Ministry of Building Construction, Research Center for Housing, Building and Physical Planning, Cairo, Egypt, 2018.
- [13] A. A. KHALIL, T. F. EL-SHAFIEY, M. HUSSEIN AND A. T. BARAGHITH (2014),"Shear behaviour of high performance reinforced concrete beams", April 2014
- [14] ACI Committee 318. (2014). Building Code Requirements for Structural Concrete (ACI 318M-14) and Commentary (318R-14). Farmington Hills, MI: American Concrete Institute. Abaqus/CAE 6.14 User's Manual